Thermographic application of black coatings on metals

by D. Legaie*, H. Pron*, C. Bissieux*, and V. Blain**

* Laboratoire de Thermophysique (URCA/GRESPI/LTP), UFR Sciences Exactes et Naturelles, University of Reims Champagne-Ardenne, Reims, France
** Centre régional d'Innovation et de Transfert de Technologie – Zone de Haute Technologie du Moulin Leblanc, Charleville-Mézières, France

Abstract

The aim of this work is the study of two black coatings: a spray of black paint, an amorphous carbon film deposited by magnetron sputtering. Our interest in such films is motivated by research on coatings with an homogeneous thickness realized at low temperature in order to characterize steels. The thermophysical properties are measured by means of lock-in photothermal thermography. An analytical study in the Hankel domain is performed, based on the study of heat transfer in the infrared sequences. For thermographic application on metals, using a thin film of carbon appears more favourable.

1. Introduction

For thermographic studies, surfaces of samples are frequently blackened with "black coatings" [1,2,3] in order to enhance and homogenize their absorptivity and emissivity. Following applications, engineers can choose from a variety of black coatings, however the black paint technique [4,5] is widely used. Indeed, the black paint spray can be applied at room temperature and it is fast to realize. Usually, to ensure the opacity of this layer, the thickness coating is greater than 20µm.

Thus, to characterize a 316L steel by photothermal infrared thermography, a KrylonTM black paint layer has been applied on this substrate. An analytical model based on the Hankel transform and simulating the heat transfer has been implemented. Then, an analysis in the Hankel domain has been realized. The results show that the coating thickness can be critical for adequate performance. In fact, on the one hand, the model is very sensitive to the value of this variable. On the other hand, the thickness coating seems too important to identify the thermal properties of the substrate. So, to characterize the substrate with this technique, it is necessary to find a thinner black coating.

Since the carbon or graphite [6] particles are the pigments [7] responsible for opacity and color of the black paint, a carbon deposit could be an alternative to the black paint. Consequently, in a second step, a study on an amorphous carbon thin film deposited by DC magnetron sputtering has been realized. With a thickness coating about 1µm, the sensitivity curves in the Hankel domain prove that the model becomes strongly sensitive to the thermal conductivity of the steel substrate 316L. Finally, a parameter identification using a Gauss-Newton algorithm allowed to estimate with a good accuracy the thermal conductivity of this substrate.

2. Experimental set-up

The technique applied here is photothermal infrared thermography under modulated laser irradiation. A paint layer is sprayed on a steel substrate 316L (thickness: 2.5mm, ρ=7950 kg.m-3, thermal conductivity: k=15W.m-1.K-1, specific heat: Cp=500J.kg-1.K-1). The sample surface is heated by a diode pumped YAG laser (DPSS) at the 532nm wavelength. The modulation of the laser beam is realized by an acousto-optic modulator driven by a sinusoidal function under LabviewTM program. For the lock-in procedure a photodiode gives the reference signal allowing amplitude and phase measurements. An infrared camera, CEDIP IRC 320-4LW, records series of images of the thermal responses. The measurements are run under computer control and the program, under LabviewTM, allows the numerical lock-in detection [8] of real and imaginary parts of the complex temperature.
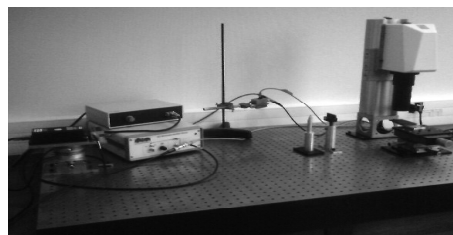

Fig. 1. *Experimental set-up*

3. Estimation procedure

Following the approach proposed by Maillet et al. [9], we present an analytical model using Hankel transform and a procedure for parameter estimation in the transform space.

3.1 Theoretical model

The thermal problem can be written by using the heat diffusion equation for a bi-layer medium and assuming the geometry as 2D axis-symmetrical:

$$\frac{\partial^2 T(r,z)}{\partial r^2} + \frac{1}{r}\frac{\partial T(r,z)}{\partial r} + \frac{\partial^2 T(r,z)}{\partial z^2} - \frac{jw}{a}T(r,z) = -\frac{q(r,z)}{k}$$

(1)

The thermal response can be searched as Green Harmonic Functions [10,11]:

$$\frac{d^2 H(\lambda,z|z')}{dz^2} - \sigma_i^2 H(\lambda,z|z') = -\frac{\delta(z-z')}{k}$$

(2)

Then, the Hankel transform of the temperature in the layer 1 (black coating) is expressed as:

$$\overline{T_1}(\lambda,z) = \int_0^l H_{11}(\lambda,z|z')\overline{q_1}(\lambda,z')dz' + \int_l^d H_{21}(\lambda,z|z')\overline{q_2}(\lambda,z')dz'$$

(3)

The following boundary and interface conditions are considered for computing the solution:
- At the surface of the black coating (z=0):

$$k_1 \left.\frac{\partial T_1(r,z)}{\partial z}\right|_{z=d} = h_1 T_1(r,z)\big|_{z=d}$$

(4)

- At the rear face of the sample(z=d):

$$-k_2 \left.\frac{\partial T_2(r,z)}{\partial z}\right|_{z=d} = h_2 T_2(r,z)\big|_{z=d}$$

(5)

- Continuity of heat flux at the interface between substrate and black coating (z=l):

$$-k_1 \left.\frac{\partial T_1(r,z)}{\partial z}\right|_{z=l} = -k_2 \left.\frac{\partial T_2(r,z)}{\partial z}\right|_{z=l}$$

(6)

- Perfect contact between the coating and the substrate:

$$T_1(r,z)\big|_{z=l} = T_2(r,z)\big|_{z=l}$$

(7)

The analytical expression of each source transform can be written as:

$$\overline{q_1}(\lambda,z) = \frac{(1-\rho)P\beta_1}{4\pi}\exp\left[-\left(\frac{\lambda r_0}{2}\right)^2\right]\exp\left[-\beta_1 z\right]$$

(8)

$$\overline{q_2}(\lambda,z) = \frac{(1-\rho)P\beta_2}{4\pi}\exp\left[-\beta_1 l\right]\exp\left[-\beta_2(z-l)\right]\exp\left[-\left(\frac{\lambda r_0}{2}\right)^2\right]$$

and

(9)

3.2 Determination of the thermal response centre

The detector pixels are naturally arranged in a Cartesian system of coordinates. However, in order to take advantage of the axial symmetry, the pixels need to be replaced as a function of their radial position. This locating must begin by the map centre determination.

To determine the centre of the intensity distribution supplied by the matrix detector, a Gaussian fit approach has been used on experimental amplitude images as given by the lock-in procedure.

Every pixel of coordinates (xi, yj) has an intensity value L(xi, yj).

The distribution is considered as a spread function with a point source. The limited image is fitted with a bidimensional Gaussian function [12]:

$$L(x,y) = Ae^{-\frac{(x-x_0)^2+(y-y_0)^2}{2\sigma^2}}$$

(10)

where A is the amplitude, σ is the width parameter of the radial symmetrical Gaussian profile and (x0,y0) are the centre coordinates.

The algorithm uses a Levenberg-Marquardt fitting method. The estimation results are extremely accurate even if the image is disturbed with a great amount of measurement noise.

Once the centre of the thermal response map is located, it is possible to calculate all the effective radius separating the centre of each pixel and the centroïd, then to rebuild the temperature profile.

3.3 Evaluation of the discrete Hankel transform of the data

The discrete Hankel transform of the temperature data series is expressed as:

$$T^*(\lambda, z) = \frac{2}{r_0^2} \sum_i T(r_i, z) J_0(\lambda r_i) r_i \Delta r_i$$

(11)

corresponding to the normalized continuous transform:

$$T^*(\delta, z) = \frac{\int_0^\infty T(r,z) J_0(\delta r) r \, dr}{\int_0^\infty e^{-\left(\frac{r}{r_0}\right)^2} r \, dr} = \frac{2}{r_0^2} \int_0^\infty T(r,z) J_0(\delta r) r \, dr$$

(12)

Practically, the Hankel transform is evaluated here at the layer surface (z=0). However, the radius step Δr_i is non-constant here. So, a numerical method of integration using an approximation polynomial is necessary. The general method to evaluate the integral of a function f(x) on an interval [x0, xm] from discrete values yi = f(xi), can be described as:

$$\int_{x_0}^{x_m} f(x) dx = \sum_{i=0}^{i=n} a_i f(x_i)$$

(13)

This numerical integration has been realized by using a dedicated "toolbox" available in MathematicaTM.

3.4 Identification in the Hankel space

3.4.1 *Spatial frequency band and sampling step definitions*

Let u and v be the classical Fourier variables, that are the spatial frequencies along x and y. Since $\lambda^2 = 4\pi^2(u^2 + v^2)$ [13], we chose umin corresponding to the inverse of the window width during the recording process by the infrared camera and umax to the inverse of the inter-pixel length; then $\delta min = 2\pi\sqrt{2}$ umin and $\delta max = 2\pi\sqrt{2}$ umax. In this way, we attempted to take into account the classical sampling problems (aliasing, under-sampling, windowing).

Here, δmin = 3,000 m-1 and a sampling step $\Delta\delta$ of 100 m-1 have been chosen. The sampling in the real space is here close enough to ensure δmax = 300,000 m-1, far away from the useful frequency range (even applying Shannon's criterion : δmax = 150,000 m-1).

3.4.2 *Gauss estimation procedure*

For the inverse problem considered here, a Gauss-Newton parameter estimation is used, about which complete relevant information can be found in Beck and Arnold [14].

The technique is based on the minimization of the difference between the measured and the corresponding theoretical values, as calculated by the mathematical model.

The estimation of $\vartheta = [\vartheta_i]_{i=1}^p$ consist in minimizing the Ordinary Least Square criterion:

$$S(\vartheta) = \sum_{j=1}^n \left(T^*_{discrète} - \overline{T}(\vartheta)\right)^2$$

(14)

where θi is the ith paramater for estimation and $T^*_{discrete}$ is the matrix of discrete values of the Hankel temperature [n x 1] calculated by using the measured temperature and the model solution. $\overline{T}(\vartheta)$ being not linear with respect to θ, the minimum $\hat{\vartheta} = \arg\min S(\vartheta)$ is computed according the Gauss Newton algorithm. The iterative process is described in [14].

4. Black paint coating

4.1 Sample preparation

The black paint used was the Ultra Flat Black paint KrylonTM. It has been applied from aerosol spray on the steel substrate 316L, at room temperature. The distribution of this coating being not strictly uniform, the value admitted for the coating thickness is an average of 10 measurements. For the measurement, a POSITECTOR 6000, allowing a resolution of 1μm, gives a mean value around 18μm.

4.2 Estimation possibilities

Some parameters of the model can be estimated easier than others, so the sensitivities to the unknown parameters have to be calculated. On the one hand, they give information on the identification feasibility then, on the other hand, they play an important role in the identification procedure. Sensitivities to the most important parameters are investigated.

The main ones are the thickness (l) , the thermal conductivity (k1), the optical absorption coefficient (β1) of the coating and the thermal conductivity (k2) of the substrate.

A qualitative study has been realized using the reduced form of the sensibility coefficient, which is usually defined as:

$$X_{ji}^{*} = \vartheta_i \frac{\partial \overline{T}_j}{\partial \vartheta_i}$$

(15)

where $\overline{T}$ is the value of the Hankel transform of the temperature calculated by the model, n is the number of measured values, θi is the ith paramater for estimation (i=1,…, p)and p is the number of parameters under estimation.

The sensitivity curves show that the reduced sensitivities on the imaginary part are much weaker than those to the real part. Among the four parameters selected, it appears that the deposit thickness is the most influent on estimation results. Moreover the curves show that in this configuration where the coating thickness is almost 20μm, the model has little sensitivity to the thermal conductivity (k2) of the substrate. However, the optical absorption (β1) and the thermal conductivity (k1) of this coating are not correlated. Thus, it is possible to realize a simultaneous estimation of these two parameters on the spatial frequency domain.
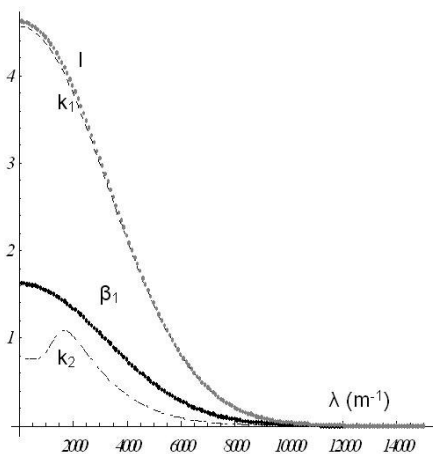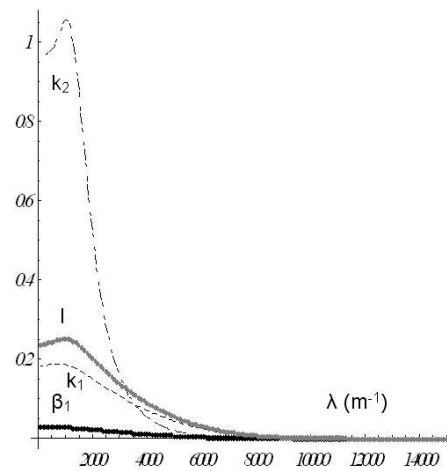

Fig. 2. *Sensitivities of the real part*   **Fig. 3.** *Sensitivities of the imaginary part*

4.3 Optical and radiative characterization

Infrared reflectance measurements have been recently reported about Krylon films [15] but do not allow enough accurate computation of the reflectivity. Influence of the infrared spectral emissivity of films has been shown [16,17,18]. Here, we considered the Krylon film as opaque in the long wave domain, since we tested samples covered with different thicknesses of Krylon paint, and found no variation of emissivity from 20 to 40μm.

4.4 Thermal conductivity identification of the black paint layer

The experiment is composed of more than 200 images of 160x120 pixels sampled at 50Hz, at a modulation frequency of 1Hz. This single frequency has been chosen here as a compromise between the intensity of the signal and its sensitivities to the different parameters.

Once both amplitude and phase maps are obtained, the complex temperature profile as a function of the effective radius is built.
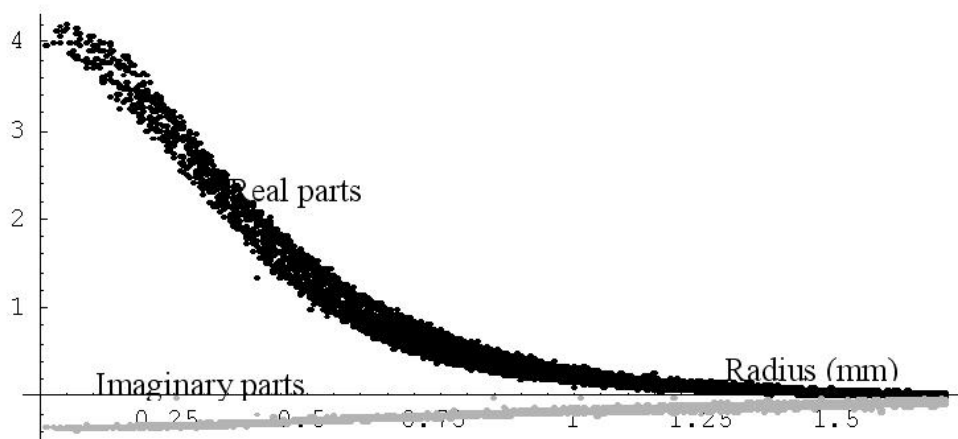
Fig.4. Rebuilt temperature profile (316L steel + 18µm black paint)

The result of the fit on the experimental measurements in the Hankel space is shown figure 5. It appears that the fit is always better on the real part than on the imaginary part. The oscillations on the imaginary part clearly show the convolution effects of the windowing in the Hankel space.
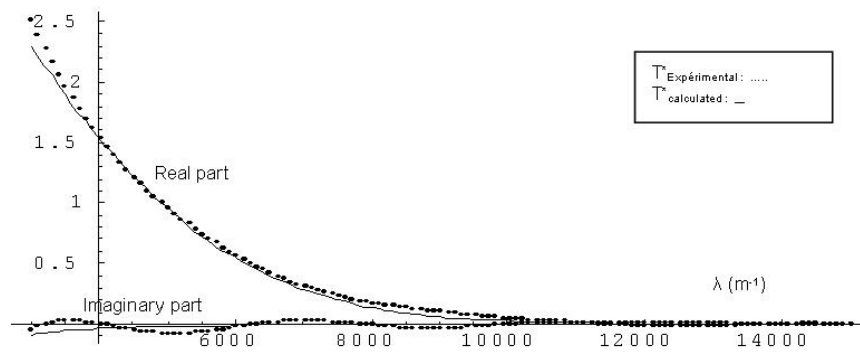

Fig.5. Experimental and calculated profiles (316L steel + 18µm black paint)

Several authors have already tried to estimate the thermal properties of black paint coating on a metallic backing [19].

Here, we found a thermal conductivity for the Krylon™ black paint: k1=0.152±0.025 W.m-1.K-1 and an optical absorption coefficient : $\beta 1$ = (10±2). 104 m-1. In the literature, some estimations of the thermal diffusivity already exists for this paint. However the values are very different: for Atalla [20], at 60°C, $\alpha 1$ = 1.78×10-8 m2.s-1 (with $\alpha 1$ = k1 / (ρCp)) and for Decker et al. [21], at 1 bar, $\alpha 1$ = 1.7×10-7 m2.s-1 and at 2 bar, $\alpha 1$ = 2×10-7 m2.s-1. In the present work, the black paint layer diffusivity is found to be $\alpha 1$ = 0.15/(2×106) = 7.5×10-8 m2.s-1.

It is pointed out that the confidence intervals given here concern only the fitting procedure.

5. Amorphous carbon thin film

5.1 Deposition process

The amorphous carbon thin films described here were deposited by reactive dc magnetron sputtering [22] and the target had a purity at least about 99,99%. The substrates were located 7cm above the target on a rotary platform. The sputtered atmosphere was a mixture of argon and hydrogen. During the process, the vacuum pressure was 3.2 10-3mbar and the sample temperature was 400°C. The discharge was sustained with a power of 5kW. The thickness of the film, determined with a resolution of 0,05µm by using a surface profilometer, was near 1µm.
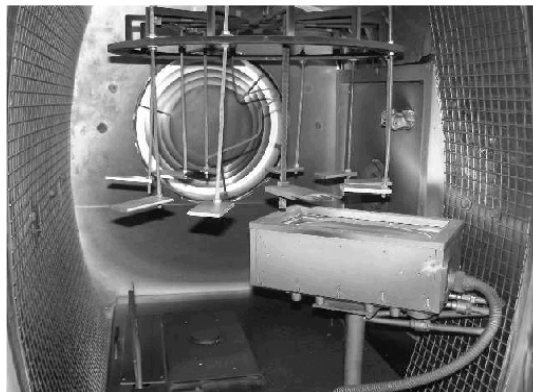
Fig. 6. *Deposition chamber*

5.2 Sensitivity study

Regarding the amorphous carbon thin film, the thermophysical properties have been found in the literature (k=1.6 W.m-1.K-1; ρ=1950 kg.m-3; Cp=710 J.kg.K-1) [23]. The rotation of the platform guarantees a thickness uniformity better than 5% [24] and the value of the deposit thickness is near 1μm.

The sensitivity study shows that around this coating thickness, the model is not sensitive to the coating properties but to the substrates properties. Then, this technique should allow the characterization of the substrate, without knowing precisely the thermal properties of the coating.
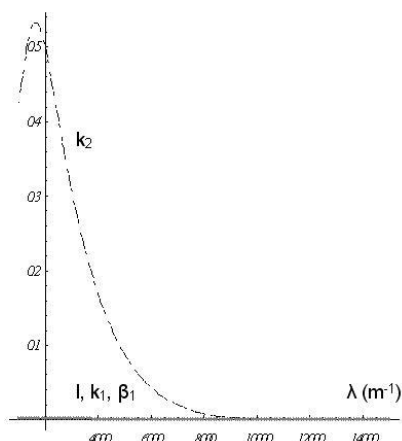

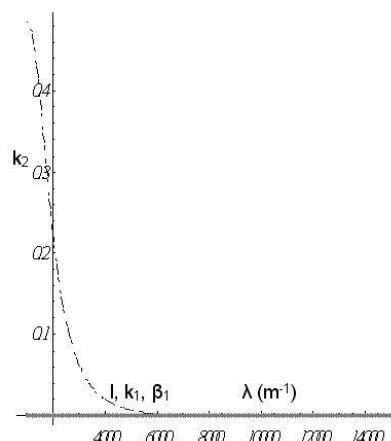**Fig.5.** *Sensitivity of the real part*

Fig.6. *Sensitivity of the imaginary part*

5.3 Optical and radiative characterization

The carbon film has different properties depending on the deposition method. In many papers, it has been shown that the a–C films are mainly determined by the substrate temperature and the particles energies during the condensation [25].

Here, two important parameters are the magnetron power (Pmagnetron=5kW) and the sample temperature during the process (Tsample=400°C). The optical indexes necessary for the radiative characterization were found in the literature [22, 26, 27].

In the visible spectrum, the optical indexes are n=1.8 (refraction index) and g=0.72 (extinction index). With these values, and for a thickness of 1μm, the optical thickness calculations show that the coating can be considered as opaque. In the far infrared spectrum, the optical index becomes n=2.38 and g=0.65. The layer appears here to be semi-transparent. Then, a correction could be applied to the experimental values, the multiplying factor being the global emissivity of the sample.

In order to determine the value of this parameter, an experimental method has been applied. It consists in raising the temperature of a sample recovered partially with two coatings, the emissivity of one of them being known. The infrared camera records the radiative intensities.

On the amorphous carbon part of the sample, at 50°C:

$$L_{measured-Carbon} = \varepsilon_{sample} L^0\left(T_{sample}\right) + \left(1 - \varepsilon_{sample}\right) L_{environment}$$

(16)

On the black paint part of the sample, at 50°C:

$$L_{measured-Black-paint} = \varepsilon_{Black-paint} L^0\left(T_{sample}\right) + \left(1 - \varepsilon_{Black-paint}\right) L_{environment} \tag{17}$$

Then the emissivity of the sample with its amorphous carbon coating is derived from:

$$\varepsilon_{sample} = \frac{L_{measured-Carbon} - L_{environment}}{L^0\left(T_{sample}\right) - L_{environment}} \tag{18}$$

with:

$$L^0\left(T_{sample}\right) = \frac{L_{measured-Black-paint} - \left(1 - \varepsilon_{Black-paint}\right) L_{environment}}{\varepsilon_{Black-paint}} \tag{19}$$

Using this experimental method, the emissivity was evaluated here at 0.89.

5.4 Thermal conductivity identification of 316L steel substrate

The Gauss-Newton algorithm converges easily towards a unique value. The result of adjustment is shown in figure 7. With this method, the thermal conductivity of 316L steel substrate is estimated to be : k2 = 14.2 ± 0.9 W.m-1.K-1.

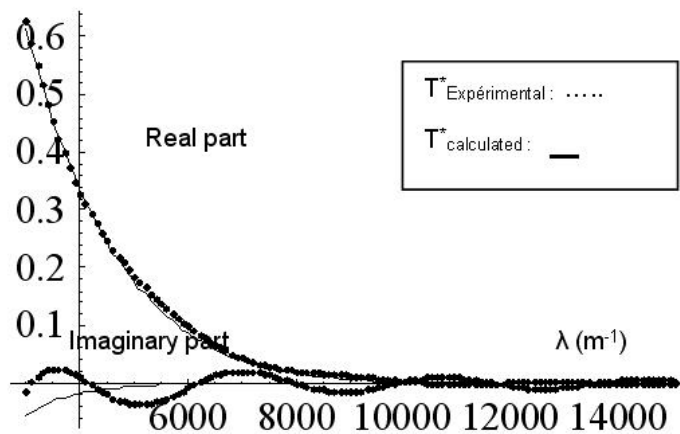**Fig.7.** *Experimental and calculated profiles (316L steel + 1µm of amorphous carbon film)*

6. Conclusion

The identification from theoretical and experimental spatial frequency profiles in the Hankel domain has allowed a convenient way for the estimation of the thermophysical properties of layers on steel substrate. Identification of the thermophysical properties of the sprayed black paint Krylon well succeeded.

Preliminary studies have been realized with amorphous carbon coatings, before undertaking the identification of thermophysical properties of metals under such this films. This coating reveal to be sufficiently thin (around 1µm) and conducting, in order to bring far better sensitivities to the metal substrate properties, when compared with those to the paint layer properties. Indeed, it is very uniform across the sample surface. However, depending on the deposition process, the layer could become semi-transparent in the infrared range, requiring the determination of the sample global emissivity. The main advantage of the amorphous carbon coating is the low sensitivity of the photothermal method to its own thermal properties.

REFERENCES

[1]   D.B. Betts, F.J.J. Clarke, L.J. Cox, and J.A. Larkin. Infrared reflection properties of five types of black coating for radiometric detectors, J.Phys.E: Sci.Instrum., 18 (1985) 689-696.
[2]   W.R. Blevin, and W.J. Brown. Black Coatings for Absolute Radiometers, Metrologia, 2 (1996) 139-143.
[3]   M.R. Dury, T. Theocharous, N. Harrison, N. Fox, and M. Hilton. Common black coatings – reflectance and ageing characteristics in the 0.32-14.3µm wavelength range, Optics Communications, 270 (2007) 262-272.
[4]   M.J. Persky. Review of black surfaces for space-borne infrared systems, Review of Scientific Instruments, 70 (1999) 2193-2217.
[5]   I. Mellouki, N. Bennaji, and N. Yacoubi. IR characterization of graphite black-coating for cryogenic detectors, Infrared Physics & Technology, (2006).

[6]   I. Mellouki, O. Touayar, T. Ktari, and N. Yacoubi. Deposition and characterization of graphite-black coating for absolute pyroelectric detectors, Infrared Physics & Technology, 45 (2004) 273-279.

[7]   D.M. Hyde, and S.M. Brannon. Investigation of Infrared Reflective Pigmentation Technologies for Coatings and Composite Applications, COMPOSITES 2006, St. Louis, MO USA, October 18-20, 2006.

[8]   H. Pron. Applications des effets photothermiques et thermomécaniques à l'analyse des contraintes appliquées et résiduelles, thesis, Université de Reims, France (2000).

[9]   D. Maillet, J.C. Batsale, A. Bendada, and A. Degiovanni. Integral methods and nondestructive testing through stimulated infrared thermograpgy, Int. J. Thermal Sciences, 35 (1996) 14-27.

[10] Y. Gillet, and C. Bissieux. Diffusion harmonique de la chaleur appliquée au contrôle non destructif par méthodes photothermiques, Int. J. Thermal Sciences, 38 (1999) 530-540.

[11] D. Legaie, H. Pron, and C. Bissieux. Characterization of a black paint layer by photothermal lock-in thermography , Parameter identification in the Hankel space, QIRT Journal, 4 (2007) 201-218.

[12] D.D. Udrea, P.J. Bryanston-Cross, W.K. Lee, and M. Funes-Gallanzi. Two sub-pixel processing algorithms for high accuracy particle center estimation in low seeding density particle image velocimetry, Optics and Laser Technology, 28 (1996) 389-396.

[13] H. Pron, and C. Bissieux. 3D Thermal modeling applied to stress-induced anisotropy of thermal conductivity, Int. J. Thermal Sciences, 43 (2004) 1161-1169.

[14] J.V. Beck, and K.J. Arnold. Parameter estimation in engineering and sciences, John Wiley & Sons (1977).

[15] J.L. Miller. Multispectral infrared bi-directional reflectance distribution function forward-scatter measurements of common infrared black surface preparations and materials, Optical Engineering, 45 (2006).

[16] H.G. Walther, U. Seidel, W. Karpen, and G. Busse. Application of modulated photothermal radiometry to infrared transparent samples, Review of Scientific Instruments, 63 (1992) 5479-5480.

[17] U. Seidel, and H.G. Walther. The influence of the spectral emissivity on the signal phase at photothermal radiometry, Review of Scientific Instruments, 67 (1996) 3658-3663.

[18] S. Paolini, and H.G. Walther. Photothermal radiometry of infrared translucent materials, Journal of Applied Physics, 82 (1997) 101-106.

[19] O. Raghu, and J. Philip. Thermal properties of paint coatings on different backings using a scanning photo-acoustic technique, Meas. Sci. Technol, 17 (2006) 2945-2949.

[20] S.R. Atalla. The ac-Heated Strip Technique for the Measurement of the Thermal Properties of Thin Solid Nonconducting Layers, Int. J. Thermophysics, 23 (2002) 253-265.

[21] C.A. Decker, and T.J. Mackin. Measuring film thickness using infrared imaging, Thin Solid Films, (2005) 196-200.

[22] M. Rubin, C.B. Hopper, N-H. Cho, and B. Bhushan. Optical and mechanical properties of dc sputtered carbon films, J. Matter. Res., 5 (1990) 2538-2542.

[23] L.R. David. CRC Handbook of Chemistry and Physics, 78th Edition (1997-1998).

[24] M. Balden, B.T. Cieciwa, I. Quintana, E. de Juan Pardo, F. Koch, M. Sikora, and B. Dubiel. Metal-doped carbon films obtained by magnetron sputtering, Surface & Coatings Technology, 200 (2005) 413-417.

[25] A.A. Onoprienko and I.B. Yanchuk. Temperature dependence of the mechanical properties of amorphous carbon films deposited by magnetron sputtering, Powder Metallurgy and Metal Ceramics, 45 (2006) 190-194.

[26] E. Mounier. Etude des transferts de matières et d'énergie dans un réacteur de dépôt par pulvérisation cathodique et caractérisation des couches de carbone obtenues, thesis, Institut National Polytechnique de Grenoble, France (1995).

[27] E.D. Palik. Handbook of optical constants of solids. Academic Press. London (1998).